Sensors & Actuators: B. Chemical 321 (2020) 128453

Contents lists available at ScienceDirect

Sensors and Actuators B: Chemical

journal homepage: www.elsevier.com/locate/snb

Subnanomolar detection of ions using thin voltammetric membranes with reduced Exchange capacity

Kequan Xu, Gaston A. Crespo, Maria Cuartero*

Department of Chemistry, School of Engineering Science in Chemistry, Biotechnology and Health, KTH Royal Institute of Technology, Teknikringen 30, SE-100 44, Stockholm, Sweden

ARTICLE INFO

Keywords:
Ion-Selective membrane
Ion exchanger
Poly(3-octylthiophene)
Silver analysis
Limit of detection
Environmental waters

ABSTRACT

Herein, we report on a new strategy to improve the limit of detection of ionophore-based thin membranes interrogated under accumulation/stripping electrochemical protocol. Accordingly, we demonstrate subnanomolar detection of silver ion (Ag^+) in water samples by re-formulating the membrane content with a reduced amount of the cation exchanger sodium tetrakis[3,5-bis(trifluoromethyl)phenyl]borate (Na^+TFPB^-), i.e. 10 mmol kg^{-1} compared to 40 mmol kg^{-1} commonly used in previous thin cation-selective membranes. Thoughtfully, by decreasing the amount of NaTFPB in the membrane phase, a diminution of its total ion-exchange capacity is to be seen. Essentially, a lower exchange capacity causes that the saturation of the membrane occurs at a lower concentration of Ag^+, allowing us to reach a lower limit of detection. This effect is indeed promoted by achieving the total replacement of the Na^+ present in the membrane by Ag^+ entering from the solution (even at the subnanomolar level) at shorter accumulation times in the readout protocol. For the silver-selective electrode, we found a linear range of response with the peak current from 0.05–10 nM Ag^+ concentration. The developed silver-selective electrode is successfully applied to the determination of Ag^+ at the (sub)nanomolar level in different water samples (i.e., tap water, seawater and freshwater samples), with the results validated using inductively coupled plasma mass spectrometry as well as recovery studies. In addition, the electrode is suitable for dynamic studies involving the interaction of Ag^+ with compounds forming natural organic matter in aquatic resources such as humic acid.

1. Introduction

Today, there is an increasing environmental concern about water discharges comprising silver ions (Ag^+). Despite the risk to aquatic organisms by Ag^+ exposure being clear, the toxicity level and targeted specie strongly depend on the silver speciation [1,2]. For example, it has been demonstrated that Ag^+ is toxic to specific bacteria but, besides that, Ag^+ may interact with other chemicals potentially increasing its environmental impact. This is the case of the reaction with natural organic matter (NOM), which is known to disrupt the normal balance of the aquatic ecosystem; and with Cl^- to form complexes such as $AgCl_2^-$, $AgCl_3^{2-}$, and $AgCl_4^{3-}$, which are also toxic to fishes [3,4]. Accordingly, the monitoring of Ag^+ content in water but also reactivity studies are essential for the appropriate assessment of its toxicity and accumulation in the water landscape. In this regard, ion-selective electrodes (ISEs) offer an excellent option to measure Ag^+ in water in a fast, easy, inexpensive and reliable way besides compatibility with in situ measurements [5]. This is the reason for the extensive research accomplished on silver-selective electrodes for water analysis up to date.

The very first potentiometric membrane-based silver-selective electrode was demonstrated in 1986 by Lai and Shih and comprised a dithia crown ether as selective receptor (called as ionophore in the ISE jargon) [6]. Other ISEs based on different kinds of ionophores have been also published, highlighting the following contributions to date. (i) In 1994, Reinhoudt and co-workers reported on a thioether-functionalized calixarene that is currently the most widely used (and commercially available, i.e. silver ionophore IV in Sigma Aldrich) silver ionophore, as far as we know [7]. (ii) Electrodes based on thiocarbamate derivatives [8,9] and thiaazacrown ethers [10] demonstrated limits of detection in the nanomolar range and even lower, when silver fluxes across the membrane were specifically controlled. This can be achieved following different strategies. For example, by tuning the composition of the inner-filling solution as well as the membrane conditioning [10,11]. Then, in all-solid-state ISEs, plasticizer-free membranes based on methylmethacrylate–decylmethacrylate

* Corresponding author.
E-mail address: mariacb@kth.se (M. Cuartero).

https://doi.org/10.1016/j.snb.2020.128453
Received 11 May 2020; Received in revised form 9 June 2020; Accepted 10 June 2020
Available online 20 June 2020

copolymer were used to provide small ion diffusion coefficients, additionally improving the limits of detection [9]. (iii) Interestingly, the 'conditioning strategy' was further applied to fluorous membranes doped with (perfluorodecylethylthiomethyl)benzene as ionophore, reaching a limit of detection in the range of 4×10^{-11} M [12].

Up to now, all the reported silver-selective electrodes truly demonstrated suitability for the analysis of real water samples in centralized laboratories, even at the subnanomolar concentration level. However, the complex procedure for electrode preparation and membrane conditioning requirements largely impeded its use for on-site as well as dynamic measurements in real contexts. On the other hand, undoubtedly, the exhaustive research on controlled ion-transfer processes across the membrane has open up new possibilities towards a future decentralized analysis of Ag^+ among other trace metals [13,14]. This path is expected to bring unique advantages related to real time detection, fast data accessibility and higher accuracy (no need of sample handling) [15]. Other crucial element in ISEs that permits facing this challenge is the solid-contact ion-to-electron transducer: since conducting polymers were introduced to the field, ISE history positively evolved towards new analytical applications thanks to the suppression of the inner filling solution [5,16–22]. Undoubtedly, one of the most used conducting polymer in ISEs is poly(3-octylthiophene) traditionally dubbed as POT, which has been reported as appropriate material for many different ISEs [21,23–25], even including silver-selective electrodes with limit of detection in the micromolar range [26,27].

In the direction of providing new sensing strategies further compatible with decentralized Ag^+ measurements, very thin silver-selective membranes have been recently interrogated with an accumulation/stripping electrochemical method [28]. This concept allows for the easy fabrication of the electrode, without the need of any conditioning step and presenting a limit of detection in the nanomolar range (i.e. 5 nM Ag^+ concentration). Thus, the preparation of the electrode was accomplished on the basis of commercial glassy carbon substrate modified with a layer of electropolymerized POT. Then, the POT-based electrode was customized with a silver-selective membrane comprising polyvinylchloride (PVC) as the polymer, bis(2-ethylhexyl)sebacate (DOS) as the plasticizer, sodium tetrakis[3,5-bis(trifluoromethyl)phenyl]borate (Na^+TFPB–) as the cation-exchanger and the silver ionophore IV. This membrane is fabricated with a reduced thickness (ca. 230 nm), compared with that used in potentiometric experiments (hundreds of micrometers) [29,30].

In this sensor, the control of the oxidation state of the POT film allows for a quick charge distribution in the electrode that results in Ag^+ transfer at the membrane|sample interface at any convenience. In particular, Ag^+ transfer has been demonstrated owing to the gradual oxidation of the POT film to POT^+ [13]. Essentially, the formed POT^+ is paired with the anionic part of the cation exchanger ($TFPB^-$), which results in the release of Ag^+ from the membrane to the solution according to the maintenance of the electroneutrality condition of the system. The Ag^+ transfer is manifested in a gaussian-shaped voltammetric wave and the change in its peak potential, current or even charge may be used as the analytical signal for analytical Ag^+ determination [13,28].

Nanomolar detection of Ag^+ is achieved whether the described electrode is interrogated under an accumulation/stripping protocol, which was originally proposed by Amemiya and co-workers coupled to ion-transfer processes [31]. The accumulation of Ag^+ occurs at a certain applied potential that controls the oxidation state of the POT film and then, these ions are expelled from the membrane to the solution during the anodic stripping step. In fact, this latter process involves any cation in the membrane (i.e. other cations in the sample such as Na^+). As a result, the observed stripping voltammograms always displayed at least two peaks corresponding to the background cations and the Ag^+. For real samples with a complex composition in cations, the overlapping of the Ag^+ peak with that associated to the sample matrix was demonstrated to affect the measurable limit of detection of the sensor. This indeed impeded the detection of Ag^+ in water samples at concentrations lower than 5 nM [28].

We present herein a new approach that formulates thin membranes (ca. 200 nm if thickness) in defective conditions of the cation exchanger (Na^+TFPB^-): i.e., really low content compared to traditional ion-selective membranes. Essentially, the early saturation of the membrane is powered by restricting the amount of charge that the membrane is able to exchange (i.e., exchange capacity). Besides that, the large preference of the membrane for Ag^+ combined with the accumulation/stripping protocol provide a very low measurable limit of detection at the subnanomolar level, being this a consequence of the premature filling of the membrane by Ag^+ coming from the solution, as here demonstrated. Thus, the developed sensor is suitable for the analysis of Ag^+ content in a wide range of environmental water samples. Because this strategy is not limited to Ag^+, it is expected to open up a new wave of selective sensors with improved limit of detection for the analysis of other ions (such as trace metals and nutrients), in all kinds of environmental waters.

2. Experimental Section

2.1. Reagents, materials, and equipment

Aqueous solutions were prepared in deionized water (18.2 MΩ cm. Lithium perchlorate (> 98 %, $LiClO_4$), 3-octylthiophene (OT, 97 %), silver nitrate ($AgNO_3$), sodium nitrate ($NaNO_3$), high-molecular-weight poly(vinyl chloride) (PVC), bis(2-ethylhexyl)sebacate (DOS), sodium tetrakis[3,5-bis(trifluoromethyl)phenyl]borate (NaTFPB), silver ionophore IV, humic acid sodium salt, concentrated sodium hydroxide solution (conc. NaOH), acetonitrile (ACN), and tetrahydrofuran (> 99.9 %, THF) were purchased from Sigma-Aldrich. Glassy carbon GC-electrode tips (Model 6.1204.300) with an electrode diameter of 3.00 ± 0.05 mm were sourced from Metrohm (Sweden). Cyclic voltammograms were recorded with a PGSTAT128 N (Metrohm Autolab B.V., Utrecht, The Netherlands) controlled by Nova 2.0 software (supplied by Autolab). A double junction Ag/AgCl/3 M KCl/1 M LiOAc reference electrode (Model 6.0726.100, Metrohm, Switzerland) and a platinum electrode (Model 6.0331.010, Metrohm, Switzerland) were used in a three-electrode cell as counter and reference electrodes respectively. The applied potential in all the voltammograms through the paper is referred to the Ag/AgCl reference electrode. A rotating disk electrode (Model EDI 101, LANGE, Switzerland) was used to spin coat the membranes on the electrodes at 1500 rpm and also for the electrochemical measurements.

2.2. Preparation of the electrodes

The electrodes were prepared as described elsewhere, by electrodeposition of a film of POT (0.1 M OT solution in 0.1 M $LiClO_4$ and ACN background, 2 cyclic voltammetry scans, 0–1.5 V, 100 mV s^{-1} and then discharging at 0 V for 120 s) and later modification with the thin-film of the membrane (by depositing at once 25 µl of the THF-based cocktail while rotating the electrode at 1500 rpm) [28]. The absence of ClO_4^- ion in the POT layer lattice or surface was confirmed in our previous studies using synchrotron-based radiation measurements. The composition of the membrane cocktail was 30 wt% of PVC, 60 wt% of DOS, 80 mmol kg^{-1} of silver ionophore IV and 40, 20 or 10 mmol kg^{-1} NaTFPB. More specifically, for the membrane with 10 mmol kg^{-1}, ca. 30 mg of PVC, 60 mg of DOS, 6.2 mg of silver ionophore IV and 0.86 mg of NaTFPB were dissolved in 1 ml of tetrahydrofuran (THF).

3. Results and discussion

In the present paper, we explore a thin membrane film that has been formulated with reduced amount of the cation exchanger NaTFPB and isbackside contacted with a POT film. This membrane presents a lower

ion-exchange capacity, i.e., the available charge to be exchanged at the membrane|sample interface is lower compared to regular thin membranes (10 mmol kg^{-1} *against* 40 mmol kg^{-1} membrane). Indeed, it was previously demonstrated that the exchange capacity of the membrane is in direct correlation with the NaTFPB initial content: with less amount of $TFPB^-$, less amount of POT is oxidized to POT^+ and less ions can be therefore exchanged at the membrane|sample interface (lower peak current and charge of the voltammetric peak) [32].

Here, we demonstrate throughout our experiments that a lower exchange capacity represents in principle two effects in the system when interrogated under accumulation/stripping protocol. Considering silver-selective membranes, first, the Ag^+ content providing the membrane saturation is lower, as a direct consequence of having les exchangeable ions in the membrane coming from the NaTFPB. And second, the time required for an effective Ag^+ accumulation into the membrane is also lower, again the reason relies on providing less amount of exchangeable positions in the membrane to be fill in by Ag^+ from the solution. The combination of these two effects advantageously results in a reduction of the limit of detection for Ag^+, always considering a thin-layer regime for mass transport inside the membrane, as demonstrated in previous papers [13].

3.1. Investigating the effect of the reduction of the amount of ion-exchanger in the membrane

Fig. 1 depicts the mechanism hypothesizing the operation principle of a thin film of silver-selective membrane interrogated under accumulation/stripping protocol: i.e. accumulation at E_{app} = 0 V over a certain period of time and then anodic linear sweep voltammetry (ALSV). Notably, this mechanism occurs in a different extent depending on the NaTFPB amount in the membrane. In addition, to describe the mechanism, we have considered that there is always a POT^+/POT mixture initially in the electrode, which is a usual situation after every accumulation/striping round.

The application of a constant potential (E_{app} = 0 V) generates that the POT^+ initially present in the electrode quickly converts to POT, with $TFPB^-$ release from the lattice of the POT film to the membrane. Upon the driving force being electroneutrality maintenance, cations enter from the solution to the membrane, as illustrated in Fig. 1a. Depending on the Na^+/Ag^+ molar ratio in the sample, it would be only Na^+ that initially enters into the membrane or both Na^+ and Ag^+. Then, over the time in which the potential is applied, there is a gradual replacement of the Na^+ in the membrane by the Ag^+ in the solution (Fig. 1b), which is in principle favoured by the presence of the ionophore but evidently depending on the Na^+/Ag^+ molar ratio in the solution (in our experiments is millimolar versus nanomolar). It is worth mentioning that, the time required to entirely replace all the Na^+ in the membrane by Ag^+ from the solution will be shorter in a membrane with a lower $TFPB^-$ content (or lower ion-exchange capacity), simply because there is less amount of Na^+ to be replaced. This statement evidently assumes a given Na^+/Ag^+ molar ratio in the sample solution facing thin-layer membranes with decreasing NaTFPB content.

However, the extension of the overall Na^+/Ag^+ exchange in each membrane certainly depends on both the mass-transport of Ag^+ in the sample (time dependency) and the membrane selectivity (depending on the Na^+/Ag^+ molar ratio in the sample solution). As an example, considering a thin membrane containing 40 mmol kg^{-1} of NaTFPB facing nanomolar concentration of Ag^+ and millimolar concentration of Na^+, the time needed for the total filling of the membrane by Ag^+ was calculated to be within the order of tens of minutes on the basis of a common diffusional-dependent event [28,33,34]. Assuming equality on all the mentioned factors, a decrease in NaTFPB membrane content results in the improvement of the limit of detection, as evidenced in our experiments.

Regarding the stripping step (ALSV), depending on the extent of the Na^+/Ag^+ exchange in the membrane (i.e., duration of the applied constant potential), both Na^+ and Ag^+ peaks or only the peak for Ag^+ (when the membrane is saturated) will appear in the stripping voltammograms, see Figs. 1c and 1d respectively. The Ag^+ concentration at which the membrane presents the sole Ag^+ peak depends on the saturation condition and, in principle, this is expected to be lower with a lower $TFPB^-$ content in the membrane. Thus, in membranes with reduced amount of NaTFPB, we expect to have an improvement in the limit of detection as a consequence of an improved accumulation of Ag^+ at the mentioned saturation stage.

To confirm our hypothesis, first of all, membranes based on decreasing amounts of NaTFPB (i.e. 40, 20 and 10 mmol kg^{-1} of membrane) while keeping constant the amount of ionophore (80 mmol kg^{-1}) were evaluated. Figs. 2a and 2b present stripping voltammograms in 10 mM $NaNO_3$ and in a mixture of 50 nM $AgNO_3$ + 10 mM

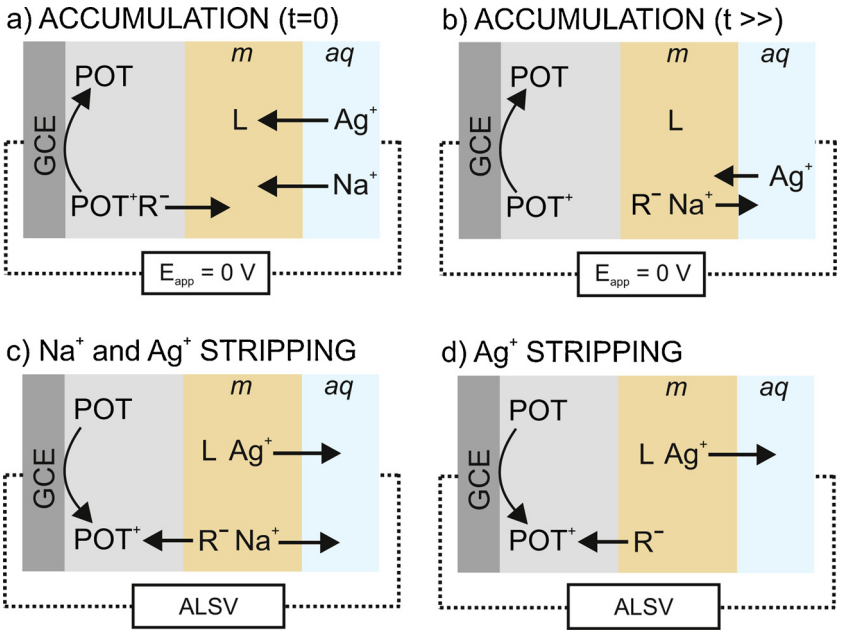

Fig. 1. Illustration of the working mechanism underlying the accumulation/stripping electrochemical protocol.

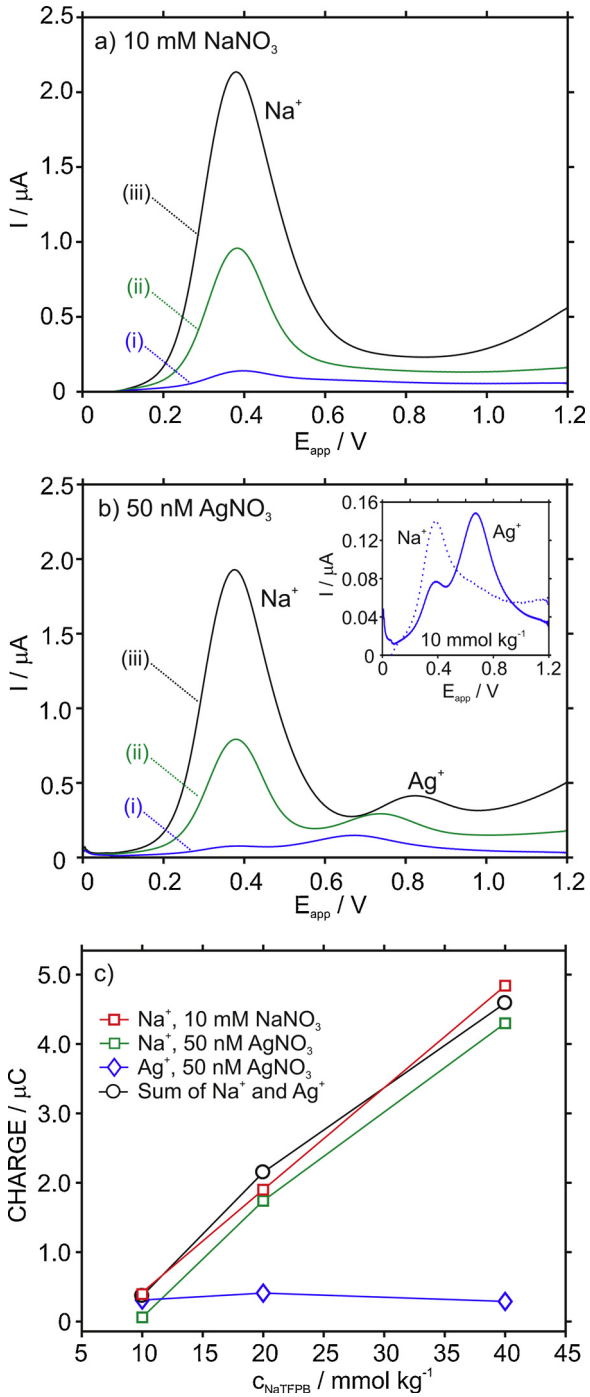

Fig. 2. Stripping voltammograms in (a) 10 mM $NaNO_3$ solution and (b) 50 nM $AgNO_3$ + 10 mM $NaNO_3$ solution. Inset: magnification of the voltammograms using the membrane with 10 mmol kg^{-1} NaTFPB interrogated under the two different protocol for comparison purposes. (c) Integrated charge for Na^+ and Ag^+ peaks. (i) Membrane with 10 mmol kg^{-1} of NaTFPB. (ii) Membrane with 20 mmol kg^{-1} of NaTFPB. (iii) Membrane with 40 mmol kg^{-1} of NaTFPB. Electrochemical protocol: E_{app} = 0 V, t_{app} = 720 s, stirring at 300 rpm, ALSV at 100 mV s^{-1}.

$NaNO_3$ solution respectively. All the membranes were tested under accumulation/stripping electrochemical protocol based on the following steps: (i) accumulation at E_{app} = 0 V during t_{app} = 720 s with external agitation at 300 rpm; and (2) anodic linear sweep voltammetry (ALSV) from 0 to 1.2 V at 100 mV s^{-1} [28]. Only the peak for Na^+ transfer (c.a. 0.4 V) was manifested in the case of $NaNO_3$ solution (Fig. 2a), since this is the only cation present in the solution. Because the ion-exchange capacity of the membrane decreases with the NaTFPB content, less cations are exchanged at the outer membrane|sample interface, as above described. Therefore, the peak charge, which reflects the exchange capacity of the membrane, expectably decreased with the NaTFPB content, see Fig. 1c.

In the 50 nM $AgNO_3$ + 10 mM $NaNO_3$ solution (Fig. 2b), Ag^+ transfer peak appeared within 0.65–0.85 V (depending on the membrane composition) together with the Na^+ peak at 0.4 V. Specifically, we found that the Ag^+ peak shifted to less positive potentials when the amount of $TFPB^-$ decreased in the membrane. The only plausible reason for this trend is that Ag^+ transfer from the membrane to the sample becomes more energetically favourable with decreasing ion-exchange capacity. Indeed, this trend corresponds with the reported behaviour for ionophore-free voltammetry thin layer membranes containing decreasing NaTFPB concentrations (Fig. 2a in reference [20].

In addition, while the peak charge for Na^+ transfer decreased with decreasing TFPB– concentration, it remained almost constant for the Ag^+ transfer, as observed in Fig. 2c. This means that the decrease in the ion-exchange capacity of the membrane, while keeping the amount of the ionophore and the same accumulation time in the electrochemical protocol, is primarily affecting to the Na^+ content present in the membrane. Accordingly, the ratio for the Ag^+/Na^+ peak charge increased from 0.05 for the membrane containing 40 mmol kg^{-1} of NaTFPB to 0.5 for 20 mmol kg^{-1} and 2.5 for 10 mmol kg^{-1}. Notably, the total charge exchanged by each membrane is rather the same regardless the tested solution (ca. 4.83, 1.92 and 0.45 for 40, 20 and 10 mmol kg^{-1}): the charge for the sole Na^+ peak in 10 mM $NaNO_3$ solution is approximately equal to the sum of those for Na^+ and Ag^+ peaks in the 50 nM $AgNO_3$ + 10 mM $NaNO_3$ solution for all the membranes, as shown in Fig. 2c. On the other hand, none of the voltammograms manifested any influence of ohmic drop as a consequence of increasing the membrane resistance with the decrease of NaTFPB amount, as demonstrated in previous studies [29].

Importantly, the peak corresponding to Na^+ transfer was remarkably suppressed in the membrane comprising the lowest $TFPB^-$ content, in principle meaning that the sole peak of Ag^+ (reflecting membrane saturation) is expected at a lower Ag^+ concentration in this membrane than in the rest. Indeed, the amount of NaTFPB in the membrane could be decreased even more pursuing the cleanest peak for 50 nM Ag^+ concentration. However, we found that membranes with a NaTFPB content lower than 10 mmol kg^{-1} displayed noisy voltammetric signals and the peaks were very small to be properly quantified, which is not very convenient for the further analytical application of the sensor. It was therefore necessary to achieve a compromise situation between the peak magnitude and noise levels while supressing the Na^+ peak as much as possible. The membrane based on 10 mmol kg^{-1} of NaTFPB provided the best results in this direction.

3.2. Facilitating silver ion accumulation in the electrochemical protocol

Next, different accumulation/stripping electrochemical protocols were evaluated to understand the need for a long accumulation step. Figs. 3a and Fig. 3b show stripping voltammograms for Ag^+ in $NaNO_3$ solution with the membranes with 40 and 10 mmol kg^{-1} and using two different accumulation protocols. The first protocol was the same one used in the previous experiments presented in Fig. 2 (i.e. E_{app} = 0 V during t_{app} = 720 s while stirring the sample at 300 rpm and ALSV). In the second protocol, the applied potential was of the same magnitude (E_{app} = 0 V), but only applied for 20 s. Then the ALSV was started after a certain time of 700 s in which the cell was kept at the open circuit potential (OCP). In other words, the ALSV is applied in both cases after 720 s (labelled as exchanging time, t_{ex}), and being the t_{app} (i.e. 720 or 20 s) the main difference.

The application of 0 V over t_{app} involves the effective conversion of POT^+ to POT after each stripping measurement, as demonstrated in our previous paper [28]. Otherwise, the spontaneous returning to the POT

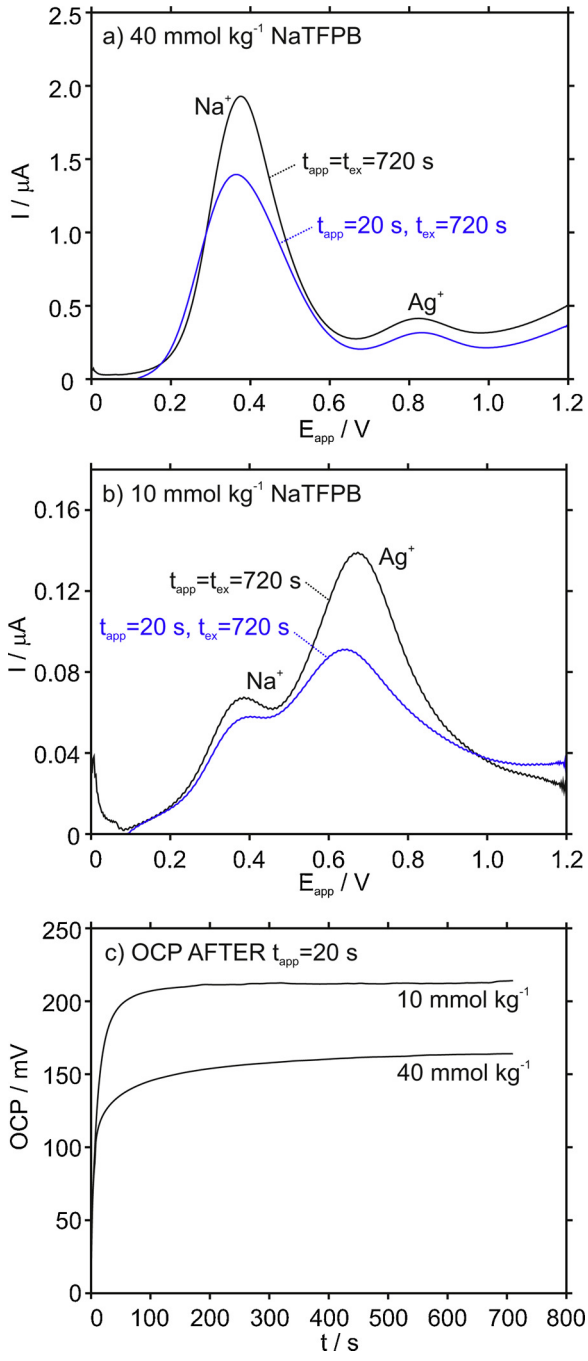

Fig. 3. Stripping voltammograms in 50 nM $AgNO_3$ + 10 mM $NaNO_3$ solution using the membrane with (a) 40 mmol kg^{-1} and (b) 10 mmol kg^{-1} of NaTFPB. (c) Evolution of the OCP over the exchange time (700 s). Accumulation protocol 1(black line): E_{app} = 0 V during t_{app} = 720 s. Accumulation protocol 2 (blue line): E_{app} = 0 V during t_{app} = 20 s and then t_{ex} = 720 s. Stirring = 300 rpm. ALSV from 0 to 1.2 V at 100 mV s^{-1} (For interpretation of the references to colour in this figure legend, the reader is referred to the web version of this article).

basal state (i.e., state at the initial OCP) takes approximately two hours. However, the experiments presented in Figs. 3a and 3b revealed that it is not necessary to hold the application of the 0 V potential for too long in order to reach POT^+ to POT conversion, meaning that the rest of the accumulation time is employed for Na^+/Ag^+ exchange in the membrane according to Fig. 1b. In this direction, despite the POT^+ to POT conversion being a fast process, we demonstrated in our previous paper that long times (in the order of 15 min) are required to have the effective accumulation of Ag^+ into the membrane: the Ag^+ peak increased for increasing accumulation time. This long time is evidently attributed now to mass-transport diffusional conditions for Ag^+ in the sample solution.

Voltammograms using the two different protocols qualitatively look the same (Figs. 3a and 3b). However, the stripping voltammograms corresponding to t_{app} = 720 s (black curves) displayed higher current and charge than those using the protocol based on a shorter applied potential of 20 s (blue curves). This is in principle expected, considering that the OCP of the electrodes subjected to the second protocol is spontaneously evolving during the t_{ex} to a value in the order of 160 and 220 mV for the membrane comprising 40 and 10 mmol kg^{-1} of NaTFPB respectively (Fig. 3c). Notably, an OCP value different than 0 V indicates that the initial state of the membrane is different after the two distinct protocols: i.e., different POT/POT^+ molar ratio and therefore, different cations' content after accumulation in the membrane. Accordingly, to have the highest peak charge, our experiments demonstrated that it is convenient to hold the E_{app} during the entire t_{ex}, i.e. $t_{ex} = t_{app}$. This protocol was selected for further experiments.

Following, we studied the evolution of the stripping peak for Ag^+ using the membrane with 10 mmol kg^{-1} of NaTFPB at different rotation speeds –with the RDE– and increasing the accumulation time. Notably, in all the experiments presented up to know, we utilized agitation with an external stirrer, but we decided to use the RDE for a meticulous adjustment of the diffusional processes involved in the accumulation of Ag^+ into the membrane (i.e. in order to optimize the experimental conditions for this process).

Fig. 4a presents stripping voltammograms for 50 nM Ag^+ concentration using increasing rotation speeds for the RDE during the accumulation step. While the Na^+ peak appeared at 1000 rpm, a sole peak of Ag^+ was displayed for higher rotation speeds: the total suppression of the Na^+ peak coming from the background solution (i.e. saturation conditions) was demonstrated with rotation speeds above 2500 rpm for the selected Ag^+ concentration. Nevertheless, very high rotation speed was not convenient because this could damage the PVC-based thin membrane through its gradual dissolution into the sample and/or detachment from the electrode surface. A similar membrane damage with the corresponding deterioration of the electrode response was previously found when the PVC thin-layer membrane was repeatedly rinsed with water [29].

Fig. 4b shows stripping voltammograms for 50 nM Ag^+ concentration using increasing accumulation times. The Na^+ peak gradually decreased with increasing accumulation time, resulting in a small shoulder of the Ag^+ peak at 180 s and totally disappearing at 720 s. These results pointed out that, with the use of the new membrane composition (10 mmol kg^{-1} of NaTFPB) and the incorporation of the RDE rather than stirring the solution, it is possible to reach the membrane saturation at 50 nM silver concentration, and using an accumulation time of just 720 s. For comparison, the saturation was achieved for 500 nM Ag^+ concentration at the optimized experimental conditions previously reported for the membrane containing 40 mmol kg^{-1} of NaTFPB [28].

3.3. Calibration graph for silver ion

Stripping voltammograms at increasing concentration of Ag^+ in the sample solution were subsequently obtained (at the optimized experimental conditions using the RDE: E_{app} = 0 V, t_{app} = 720 s, 2500 rpm and ALSV from 0 to 1.2 V at 100 mV s^{-1}). Fig. 5 depicts the observed voltammograms together with the trends of both the peak current and charge for the Ag^+ transfer. It was evident how the Na^+ peak decreased and the Ag^+ peak increased with the Ag^+ concentration (Fig. 5a). Advantageously, the first measurable Ag^+ concentration (i.e. the Ag^+ stripping peak was quantifiable) was 0.05 nM.

Furthermore, there is a linear relationship of the peak current and charge with the Ag^+ concentration in the sample. In the case of the

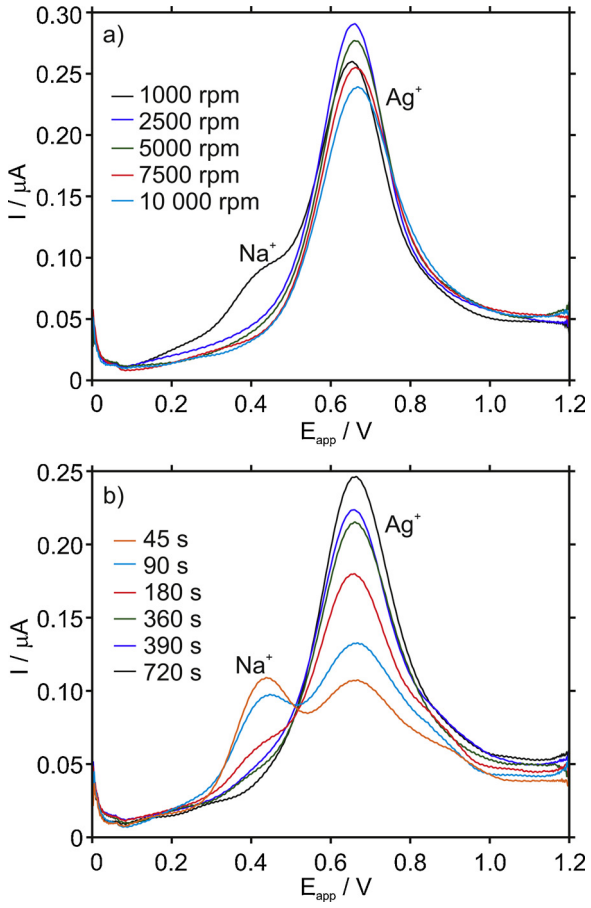

Fig. 4. (a) Stripping voltammograms in 50 nM $AgNO_3$ + 10 mM $NaNO_3$ solution at different rotation speeds of the RDE. E_{app} = 0 V, t_{app} = 720 s, ALSV from 0 to 1.2 V at 100 mV s^{-1}. (b) Stripping voltammograms in 50 nM $AgNO_3$ +10 mM $NaNO_3$ solution at different accumulation times. E_{app} = 0 V, RRDE at 2500 rpm, ALSV from 0 to 1.2 V at 100 mV s^{-1}.

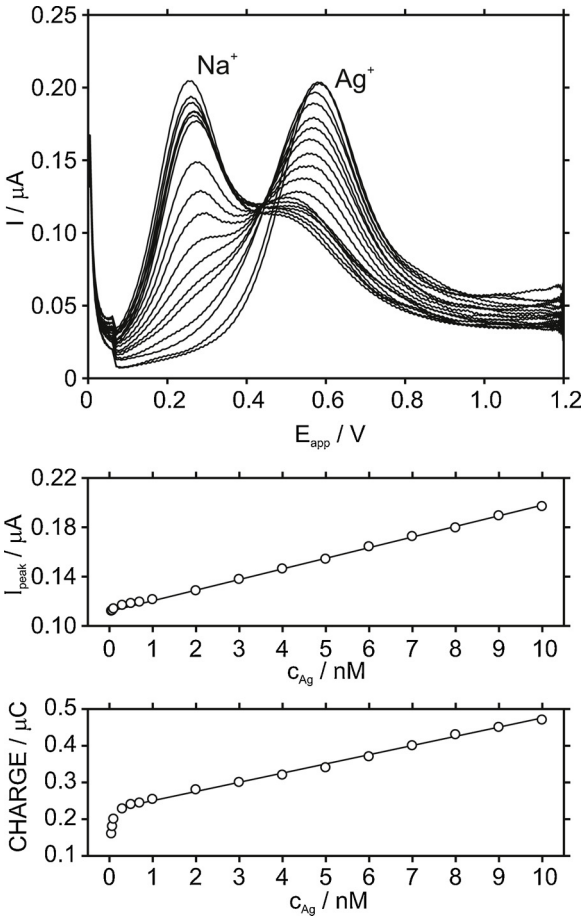

Fig. 5. (a) Stripping voltammograms in 10 mM $NaNO_3$ background solution at increasing $AgNO_3$ concentrations (0, 0.05, 0.07, 0.1, 0.3, 0.5, 0.7, 1, 2, 3, 4, 5, 6, 7, 8, 9, 10 and 20 nM). Plots of (b) the peak current and (c) charge with the Ag^+ concentration. E_{app} = 0 V, t_{app} = 720 s, RDE at 2500 rpm, ALSV at 100 mV s^{-1}.

peak current, the observed linear range was from 0.05–10 nM, coinciding with the saturation of the electrode, and the data within this range was fitted to the linear equation: $current\ (\mu A) = 84.32x10^5 \cdot c_{Ag}\,(M) + 0.11$ (r^2 = 0.9992). For the peak charge, shorter linear range was observed (from 0.3–10 nM), likely due to the difficulty in calculating the peak charge at a higher degree of overlapping between the Na^+ and Ag^+ peaks, and the data was fitted to the linear equation: $charge\ (\mu C) = 24.42x10^6 \cdot c_{Ag}\,(M) + 0.23$ (r^2 = 0.9953). The between-electrode reproducibility (n = 5) was found to be excellent, with coefficients of variation < 3% and < 7% for the slope and the intercept respectively. Signal repeatability was studied within the entire linear range of response, measuring each concentration in triplicate. For all the concentrations, we found a variation coefficient for the peak current lower than 0.5 % and lower than 1.3 % for the peak charge.

If the membrane comprising 40 mmol kg^{-1} of NaTFPB is interrogated under the electrochemical method just optimized, the first Ag^+ concentration producing a stripping voltammogram that can be quantified is 3 nM (see Figure S1a and Figure S1b in the Supporting Information). Then, the linear range of response was found to be from 5 to 60 nM for both the peak current and charge (see Figure S1c and Figure S1d in the Supporting Information). It is evident that the introduction of the RDE instead of external agitation of the solution (i.e., comparison of the experiments with the membrane containing 40 mmol kg^{-1} shown in Figure S1 and those reported in ref. [28] allows for a better control of Ag^+ diffusion in the solution and, this permits to decrease the saturation condition from 500 nM to 60 nM (ten times approx.). On the other hand, the reduction of the amount of NaTFPB in the membrane additionally decreases the saturation condition from 60 to 10 nM together with the significant improvement of the first detectable Ag^+ concentration (from 1 to 0.05 nM).

One important aspect to be considered in the response of membranes with a reduced content in NaTFPB is the role of the ionophore. It is well-known that the best composition for traditional potentiometric ion-selective membranes based on an ionophore that forms 1:1 complex with the target ion, as the case of silver-selective membrane, is that containing double molar amount of ionophore than the ion-exchanger. This is why the previous compositions tested for thin silver-membranes contained 40 mmol kg^{-1} of NaTFPB and 80 mmol kg^{-1} of silver ionophore [28].

If this philosophy is translated to our membrane based on 10 mmol kg^{-1} of NaTFPB, it would be expected that double amount of silver ionophore (i.e., 10/20 mmol kg^{-1}NaTFPB/Ionophore mmol kg^{-1}) should provide acceptable results and most likely similar to the tested membrane containing 10/80 mmol kg^{-1} NaTFPB/Ionophore. However, a membrane comprising 10/20 mmol kg^{-1} NaTFPB/ionophore presented a narrower linear range of response (3 − 7 nM against 0.05 − 10 nM), with the first detectable Ag^+ concentration being rather higher and closer to the regular membrane containing 40/80 NaTFPB/Ionophore mmol kg^{-1} in the membrane (see Figures S1 and S2 in Supporting Information). Accordingly, the amount of ionophore clearly influences the improvement of the limit of detection found for membranes with a reduced exchange capacity.

This is not the first time that the amount of ionophore incorporated into ion-selective membranes that are interrogated under a dynamic electrochemical technique is reported to modulate the linear range of response of the electrode. For example, for polypropylene-based calcium-selective membranes inspected with chronopotentiometry, wider linear range of response was demonstrated for higher ionophore concentrations [35]. Such fascinating findings may deserve more attention towards a new generation of ion-selective electrodes with tuneable analytical features. From our perspective, we consider that it is crucial to elaborate first the fundamental roots of the phenomena occurring in the membrane, which lacks in the literature, to entirely exploit the application possibilities. In this direction, and beyond the main purpose of the present paper, our research group is currently exploring the theoretical description of the response mechanism of thin membrane films considering such specific conditions that lead to lowering the limit of detection.

3.4. Detection of silver ion in environmental waters

To demonstrate the analytical applicability of the developed electrode, we determined the Ag^+ content in water samples from different sources by using the standard addition method. The peak height was selected as the analytical signal because the matrix effect generally impeded the proper calculation of the peak charge. The samples were additionally analysed by inductively coupled plasma mass spectrometry (ICP-MS) according to the procedure described in the Supporting Information. All the results are collected in Table 1.

In the case of tap water, a good correlation was found between both techniques, not only for the unaltered tap water sample but also for 0.3 nM and 0.7 nM Ag^+ additions. On the other hand, as observed in the ICP-MS results, the rest of the analysed samples comprised Ag^+ content lower than 0.1 nM or really close to this value (in the case of water from Trekanten). Thus, all these samples were out or close to the first measurable Ag^+ concentration by the developed electrode in $NaNO_3$ background (i.e. 0.1 nM Ag^+ concentration, see Fig. 5).

This fact together with possible matrix effects, that are especially significant in the case of the seawater sample, caused that it was possible to detect the Ag^+ content only in spiked samples in these cases, but also, in the original water from Trekanten. As observed in Table 1, the developed electrode is suitable for the determination of Ag^+ concentration such low as 1 nM in the seawater sample and even lower in lake samples with rather good recoveries (98–121 %). In contrast, with a bare glassy carbon electrode under anodic stripping voltammetry operation, it is possible to detect micromolar concentration of Ag^+ in freshwater and seawater [36]. Furthermore, the content in Ag^+ detected in the non-spiked Trekanten sample rather coincides for the two methods.

Fig. 6 collects some of the voltammograms of the analysed samples. The matrix effect was more evident in the case of the seawater sample (Fig. 6a). Thus, the peak corresponding to the cations in the matrix (normally appearing at 0.32 V) was overlapped to the Ag^+ peak, which indeed appeared at less positive potentials (i.e. 0.45 V) compared to that observed in $NaNO_3$ background (ca. 0.65 V).

Conversely, for the freshwater samples (Fig. 6b and Fig. 6c), the peaks for the matrix and the Ag^+ appeared quite separated. Additionally, the position of the Ag^+ peak is closer to that in $NaNO_3$ medium: 0.45, 0.55, 0.58 and 0.65 V for the seawater, the two freshwater samples and the $NaNO_3$ background respectively. As a result, it can be stated that, the more matrix effect in the sample, the less positive is the peak position of the Ag^+ transfer, likely due to a higher degree in the overlapping of all the ion transfers occurring at the membrane|-sample interface, in terms of energy. Probably, the mentioned peak overlapping could be reduced at longer accumulation times. While this will ameliorate also the limit of detection of the sensor, one drawback would be the total analysis time required for each sample.

It is not surprising that the Ag^+ content in tap water was higher than in the rest of the samples, mainly because of the presence of NOMs. Briefly, Ag^+ and other heavy metal ions (Cu^{2+}, Pb^{2+}, Cd^{2+} and Zn^{2+}) are bonded to NOM resulting in the formation of new chemical species with altered toxicity and bioavailability [37]. Notably, NOM mainly comprises humic and fulvic acids as active components [38]. Importantly, there are still open questions involving the interaction of Ag^+ and NOM: complexation kinetics and the extent of Ag^+ binding according to the NOM composition, concentration as well as any dependence with environmental changes [39]. In fact, these features are more unknown at Ag^+ nanomolar levels due to the absence of analytical tools for the dynamic monitoring of such as low concentration in the presence of NOM [39]. Advantageously, the developed silver-selective electrode is suitable for this kind of studies as following demonstrated.

Fig. 7 presents the dynamic evolution of the stripping voltammogram of a solution containing 10 nM Ag^+ concentration after the addition of 10 mg L^{-1} of humic acid. This experiment was accomplished in the presence of artificial light (bulb of 80 W). Previous to this

Table 1
Detection of silver ion content in water samples.

Sample	Added Ag^+ (nM)	Electrode			ICP-MS		
		c_{Ag} (nM)	RSD	%Recovery[a]	c_{Ag} (nM)	RSD	%Recovery[a]
Tap water	–	0.27	22.3	–	0.24	6.5	–
	+0.30	0.49	12.1	102	0.52	4.8	108
	+0.70	0.92	4.2	105	0.88	5.3	108
Baltic Sea	–	< 0.1	–	–	0.10	15.1	–
	+0.30	–	–	–	0.40	6.1	100
	+0.70	–	–	–	0.83	7.4	104
	+1.0	1.02	2.2	102	–	–	–
	+3.0	2.93	2.7	98	–	–	–
Laduviken	–	< 0.1	–	–	0.03	14.8	–
	+0.30	–	–	–	0.41	8.2	124
	+0.50	0.48	10.0	110	–	–	–
	+0.70	–	–	–	–	7.7	84
	+1.0	1.21	3.5	121	–	–	–
	+3.0	3.24	4.1	108	–	–	–
Trekanten	–	0.17	13.2	–	0.21	10.1	–
	+0.30	–	–	–	0.59	4.6	116
	+0.50	0.83	3.5	117	–	–	–
	+1.0	1.32	3.2	109	–	–	–
	+3.0	3.53	1.2	110	–	–	–

[a] The recovery percentage was calculated considering the initial amount of silver ions in the sample obtained in ICP-MS.

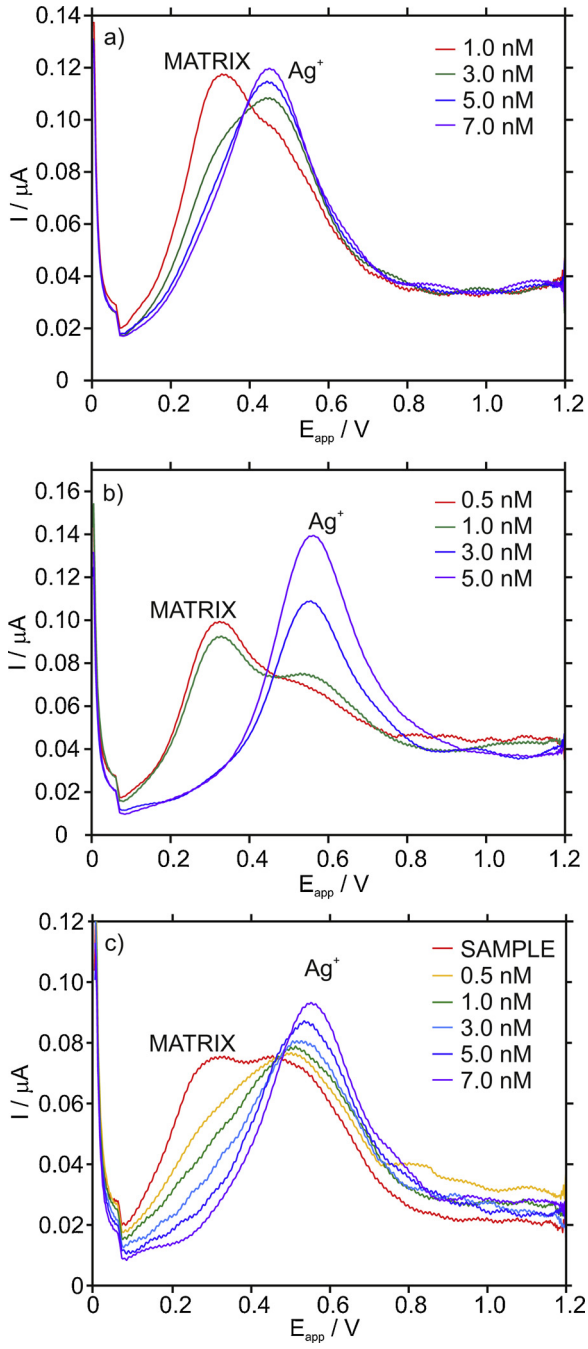

Fig. 6. Stripping voltammograms in: (a) Baltic Sea (b) Laduviken and (c) Trekanten water samples. E_{app} = 0 V, t_{app} = 720 s, RDE at 2500 rpm, ALSV at 100 mV s^{-1}.

experiment, the electrode was calibrated in the range from 0.5–10 nM Ag^+. As observed, the peak corresponding to the 10 nM Ag^+ concentration evolved to lower Ag^+ concentrations after 30 and 60 min of the addition of the humic acid. The detected Ag^+ concentration was 4.6 nM after 30 min and 1.9 nM after 60 min of reaction. Interestingly, the same experiment assessed without any artificial light, reached a constant Ag^+ concentration of 4.9 nM after 30 min of reaction. A control experiment accomplished in the presence of light and absence of humic acid revealed that the conversion of Ag^+ to Ag^0 due to light influence is negligible at the timeframe of our experiments.

Hereinafter, a much deeper study including different variables would be advantageously accessible using the developed silver-selective electrode. Thus, the evaluation of the different compounds forming

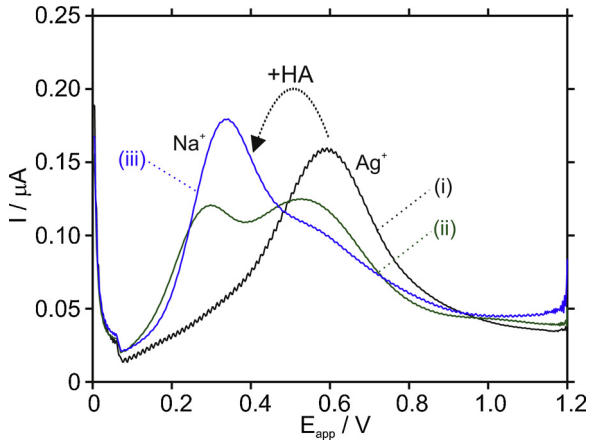

Fig. 7. Addition of humic acid (HA) to a sample comprising 10 nM Ag^+ concentration in 10 mM $NaNO_3$ background. (i) Stripping voltammogram of 10 nM $AgNO_3$ + 10 mM $NaNO_3$. (ii) Stripping voltammogram of 10 nM $AgNO_3$ + 10 mM $NaNO_3$ + 10 mg L^{-1} HA after 30 min of reaction. (iii) Stripping voltammogram of 10 nM $AgNO_3$ + 10 mM $NaNO_3$ + 10 mg L^{-1} HA after 60 min of reaction. E_{app} = 0 V, t_{app} = 720 s, RDE at 2500 rpm, ALSV at 100 mV s^{-1}.

the NOM in separate experiments would provide which is the stronger Ag^+ complexing agent. Kinetics studies at different concentrations, which were not entirely accessible up to date, could be related to toxicity effects. Finally, the influence of NOMs from different origins, short- and long-time scales, day-night cycles and different environmental conditions in the Ag^+ binding process may be also tested. Overall, a wide range of studies that can be carried out with the developed electrode is now open.

4. Conclusions

This work demonstrates the improvement of the limit of detection of thin films of cation-selective membranes, interrogated under accumulation/stripping electrochemical method, by reducing its ion-exchange capacity and keeping constant the amount of ionophore. In the case of silver-selective electrodes, the linear range of response for the peak current has to be found from 0.1–5 nM silver ion concentration, being successfully applied to silver ion detection at the (sub)nanomolar level in different water samples. In addition, the electrode is an effective tool for dynamic studies involving the interaction of silver ion with compounds (such as humic acid) forming natural organic matter in aquatic resources.

CRediT authorship contribution statement

Kequan Xu: Data curation, Formal analysis, Investigation, Resources, Software, Validation, Visualization, Writing - original draft. **Gaston A. Crespo:** Conceptualization, Funding acquisition, Methodology, Project administration, Software, Supervision, Writing - original draft, Writing - review & editing. **Maria Cuartero:** Conceptualization, Data curation, Formal analysis, Funding acquisition, Methodology, Project administration, Resources, Supervision, Validation, Visualization, Writing - original draft, Writing - review & editing.

Declaration of Competing Interest

The authors declare that they have no known competing financial interests or personal relationships that could have appeared to influence the work reported in this paper.

Acknowledgment

This project has received funding from the European Union's Horizon 2020 research and innovation programme under Marie Skłodowska-Curie grant agreement No. 792824. The authors acknowledge the additional financial support of KTH Royal Institute of Technology (K-2017-0371) and the Swedish Research Council (Project Grant VR-2017-4887). K.X. gratefully thanks the China Scholarship Council for supporting his Ph.D. studies.

Appendix A. Supplementary data

Supplementary material related to this article can be found, in the online version, at doi:https://doi.org/10.1016/j.snb.2020.128453.

References

[1] M.J. Eckelman, T.E. Graedel, Silver emissions and their environmental impacts: a multilevel assessment, Environ. Sci. Technol. 41 (2007) 6283–6289.
[2] A.M. El Badawy, T.P. Luxton, R.G. Silva, K.G. Scheckel, M.T. Suidan, T.M. Tolaymat, Impact of environmental conditions (pH, ionic strength, and electrolyte type) on the surface charge and aggregation of silver nanoparticles suspensions, Environ. Sci. Technol. 44 (2010) 1260–1266.
[3] I.L. Gunsolus, M.P.S. Mousavi, K. Hussein, P. Buhlmann, C.L. Haynes, Effects of humic and fulvic acids on silver nanoparticle stability, dissolution, and toxicity, Environ. Sci. Technol. 49 (2015) 8078–8086.
[4] H.T. Ratte, Bioaccumulation and toxicity of silver compounds: a review, Environ. Toxicol. Chem. 18 (1999) 89–108.
[5] M. Cuartero, G.A. Crespo, All-solid-state potentiometric sensors: a new wave for in situ aquatic research, Curr. Opin. Electrochem. 10 (2018) 98–106.
[6] M.T. Lai, J.S. Shih, Mercury(Ii) and silver(I) ion-selective electrodes based on dithia crown ethers, Analyst 111 (1986) 891–895.
[7] E. Malinowska, Z. Brzozka, K. Kasiura, R.J.M. Egberink, D.N. Reinhoudt, Silver selective electrodes based on thioether functionalized calix[4]Arenes as ionophores, Anal. Chim. Acta 298 (1994) 245–251.
[8] Z. Szigeti, A. Malon, T. Vigassy, V. Csokai, A. Grun, K. Wygladacz, N. Ye, C. Xu, V.J. Chebny, I. Bitter, R. Rathore, E. Bakker, E. Pretsch, Novel potentiometric and optical silver ion-selective sensors with subnanomolar detection limits, Anal. Chim. Acta 572 (2006) 1–10.
[9] K.Y. Chumbimuni-Torres, N. Rubinova, A. Radu, L.T. Kubota, E. Bakker, Solid contact potentiometric sensors for trace level measurements, Anal. Chem. 78 (2006) 1318–1322.
[10] S.G. Sang, C.W. Yu, N. Li, Y.X. Ji, J. Zhang, Characterization of a New Ag +-Selective Electrode with Lower Detection Limit, Int. J. Electrochem. Sci. 7 (2012) 3306–3313.
[11] Z. Szigeti, T. Vigassy, E. Bakker, E. Pretsch, Approaches to improving the lower detection limit of polymeric membrane ion-selective electrodes, Electroanal 18 (2006) 1254–1265.
[12] C.Z. Lai, M.A. Fierke, R.C. da Costa, J.A. Gladysz, A. Stein, P. Buhlmann, Highly selective detection of silver in the Low Ppt Range with ion-selective electrodes based on ionophore-doped fluorous membranes, Anal. Chem. 82 (2010) 7634–7640.
[13] D.J. Yuan, M. Cuartero, G.A. Crespo, E. Bakker, Voltammetric Thin-Layer Ionophore-Based Films: Part 1. Experimental Evidence and Numerical Simulations, Anal. Chem. 89 (2017) 586–594.
[14] S. Amemiya, J. Kim, A. Izadyar, B. Kabagambe, M. Shen, R. Ishimatsu, Electrochemical sensing and imaging based on ion transfer at liquid/liquid interfaces, Electrochim. Acta 110 (2013) 836–845.
[15] E. Bakker, Electroanalysis with membrane electrodes and liquid-Liquid interfaces, Anal. Chem. 88 (2016) 395–413.
[16] J. Bobacka, Potential stability of all-solid-state ion-selective electrodes using conducting polymers as ion-to-electron transducers, Anal. Chem. 71 (1999) 4932–4937.
[17] J. Bobacka, Conducting polymer-based solid-state ion-selective electrodes, Electroanal 18 (2006) 7–18.
[18] J. Bobacka, A. Ivaska, A. Lewenstam, Potentiometric ion sensors, Chem. Rev. 108 (2008) 329–351.
[19] E. Bakker, E. Pretsch, Modern potentiometry, Angew. Chemie Int. Ed. 46 (2007) 5660–5668.
[20] M. Cuartero, M. Parrilla, G.A. Crespo, Wearable potentiometric sensors for medical applications, SensorsBasel 19 (2019).
[21] J.B. Hu, A. Stein, P. Buhlmann, Rational design of all-solid-state ion-selective electrodes and reference electrodes, Trac-Trends in Analytical Chemistry 76 (2016) 102–114.
[22] J. Bobacka, T. Lindfors, M. McCarrick, A. Ivaska, A. Lewenstam, Single piece all-solid-state ion-selective electrode, Anal. Chem. 67 (1995) 3819–3823.
[23] J. Bobacka, M. McCarrick, A. Lewenstam, A. Ivaska, All-solid-state poly(vinyl chloride) membrane ion-selective electrodes with poly(3-octylthiophene) solid internal contact, Analyst 119 (1994) 1985–1991.
[24] A. Michalska, K. Maksymiuk, Conducting polymer membranes for low activity potentiometric ion sensing, Talanta 63 (2004) 109–117.
[25] E. Jaworska, M. Mazur, K. Maksymiuk, A. Michalska, The fate of poly(3-octylthiophene) transducer in solid contact ion- selective electrodes, Analytical Chemistryy (2018), https://doi.org/10.1021/acs.analchem.7b04233.
[26] D.J. Yuan, M. Cuartero, G.A. Crespo, E. Bakkert, Voltammetric thin-layer ionophore-based films: part 2. Semi-empirical treatment, Anal Chem 89 (2017) 595–602.
[27] M. Vázquez, J. Bobacka, A. Ivaska, Potentiometric sensors for Ag+ based on poly(3-octylthiophene) (POT), J. Solid State Electrochem. 9 (2005) 865–873.
[28] K.Q. Xu, M. Cuartero, G.A. Crespo, Lowering the limit of detection of ion-selective membranes backside contacted with a film of poly(3-octylthiophene), Sens. Actuator B-Chem. 297 (2019).
[29] M. Cuartero, G.A. Crespo, E. Bakker, Polyurethane ionophore-based thin layer membranes for voltammetric ion activity sensing, Anal. Chem. 88 (2016) 5649–5654.
[30] G.A. Crespo, M. Cuartero, E. Bakker, Thin layer ionophore-based membrane for multianalyte ion activity detection, Anal. Chem. 87 (2015) 7729–7737.
[31] Y. Kim, S. Amemiya, Stripping analysis of nanomolar perchlorate in drinking water with a voltammetric ion-selective electrode based on thin-layer liquid membrane, Anal. Chem. 80 (2008) 6056–6065.
[32] M. Cuartero, G.A. Crespo, E. Bakker, Ionophore-based voltammetric ion activity sensing with thin layer membranes, Anal. Chem. 88 (2016) 1654–1660.
[33] B. Kabagambe, M.B. Garada, R. Ishimatsu, S. Amemiya, Subnanomolar detection limit of stripping voltammetric Ca2+-Selective electrode: effects of analyte charge and sample contamination, Anal. Chem. 86 (2014) 7939–7946.
[34] A.J. Bard, L.R. Faulkner, Electrochemical Methods: Fundaments and Applications, John Wiley & Sons, New York, 2001.
[35] M.G. Afshar, G.A. Crespo, E. Bakker, Direct ion speciation analysis with ion-selective membranes operated in a sequential Potentiometric/Time resolved chronopotentiometric sensing mode, Anal. Chem. 84 (2012) 8813–8821.
[36] E.J.E. Stuart, N.V. Rees, J.T. Cullen, R.G. Compton, Direct electrochemical detection and sizing of silver nanoparticles in seawater media, Nanoscale 5 (2013) 174–177.
[37] D.M. Di Toro, H.E. Allen, H.L. Bergman, J.S. Meyer, P.R. Paquin, R.C. Santore, Biotic ligand model of the acute toxicity of metals. 1. Technical basis, Environ. Toxicol. Chem. 20 (2001) 2383–2396.
[38] R. Benoit, K.J. Wilkinson, S. Sauve, Partitioning of silver and chemical speciation of free Ag in soils amended with nanoparticles, Chem. Cent. J. 7 (2013).
[39] M.P.S. Mousavi, I.L. Gunsolus, C.E.P. De Jesus, M. Lancaster, K. Hussein, C.L. Haynes, P. Buhlmann, Dynamic silver speciation as studied with fluorous-phase ion-selective electrodes: effect of natural organic matter on the toxicity and speciation of silver, Sci. Total Environ. 537 (2015) 453–461.